Applied Surface Science 258 (2012) 9032–9040

Contents lists available at SciVerse ScienceDirect

Applied Surface Science

journal homepage: www.elsevier.com/locate/apsusc

Effect of an "in situ" hydrous strain on the ionic exchange process of dioctahedral smectite: Case of solution containing (Cu^{2+}, Co^{2+}) cations

Ramzi Chalghaf[a], Walid Oueslati[a,b,*], Marwa Ammar[a], Hafsia Ben Rhaiem[a], Abdesslem Ben Haj Amara[a]

[a] UR05/13-01, Physique des Matériaux Lamellaires et Nanomatériaux Hybrides (PMLNMH), Faculté des Sciences de Bizerte, Zarzouna 7021, Tunisia
[b] Département de Physique, Faculté des sciences de Gafsa, Campus Universitaire Sidi Ahmed Zarrouk, 2112 Gafsa, Tunisia

ARTICLE INFO

Article history:
Received 11 April 2012
Received in revised form 23 May 2012
Accepted 26 May 2012
Available online 2 June 2012

Keywords:
Wyoming montmorillonite
Disordered systems
In situ hydrous strain
Quantitative XRD analysis

ABSTRACT

This work aims at determining the effect of hydrous strain produced by a continuous, in situ, hydration–dehydration cycles, using a variation of relative humidity (%RH) rate here, variable (%RH), on the cation exchange process in the case of Na rich-montmorillonite. This goal is accomplished in two steps. First, the starting material (Na rich-montmorillonite) is reported "in situ" at variable RH values in order to prepare and characterize a final stressed product that will be used later in the selective exchange study, in the case of solution containing (Cu^{2+}, Co^{2+}). An XRD profile modeling approach is used to describe all structural changes caused by the environmental evolution of the RH rate. The quantitative analysis of XRD patterns is achieved through an indirect method, which is based on the comparison of experimental XRD patterns with calculated ones. This investigation allows us to determine several structural parameters related to the nature, abundance, size, position and organization of exchangeable cation and water molecule in the interlamellar space along the c^* axis.

1. Introduction

Smectite minerals are the most active constituents of soils and are the main component of bentonite rocks. The stuructural formula of dioctahedral alumina-smectites in the series montmorillonite beidellite is:

$(Al_{2-y}Mg_y)(Si_{4-x}Al_x)O_{10}(OH)_2\ M_{x\pm y}$, nH_2O when $y \geq x$, smectite is called montmorillonite.

Montmorillonite is a "T-O-T" clay mineral that is characterized by its capacity to exchange cations in the interlamellar space with others present in external solutions. The structure of the "T-O-T" clay mineral subgroups consisting of an octahedral sheet sandwiched by two tetrahedral sheets [1–3]. The half-cell structural formula of Wyoming montmorillonite determined by microprobe analysis [4] is as the following:

$$(Si_{3.923}\,Al_{0.077})(Al_{1.459}\,Ti^{4+}_{0.018}\,Fe^{3+}_{0.039}\,Fe^{2+}_{0.045}\,Mg^{2+}_{0.382})\,O_{10}(OH)_2$$
$$(Ca^{2+}_{0.177}\,Na^{+}_{0.027})$$

Very often isomorphic substitutions in octahedral and/or tetrahedral sheets make the clay platelets negatively charged, which is compensated by exchangeable cations.

The cation exchange capacity (i.e. CEC), makes montmorillonite a perfect Ion exchanger. As a consequence, smectite minerals have an effect on the hydration capacity of soils, contaminants and plant nutriments [5–7].

Several researches [8–13] are interested in the characterization of all physico-chemical phenomena (i.e. ionic exchange process, surface damage, modification of clay properties, adsorption phenomena, clay–water interface, etc.), which appear when montmorillonite is in contact with the heavy metal solution and waste water constituents, coming from its surrounding environment. Claret et al. [8] show the irreversible confinement possibility of heavy metal cation in the most active soil fraction (i.e. clay mineral) and the influence of organic matter on clay mineral evolution. Oueslati et al. [11] investigates the effect of exchangeable cation nature and abundance on the cationic exchange process in the case of di octahedral smectite and demonstrates the influence of the solution species abundance on the intrinsic selective exchange capacity (SEC). Moreover, they show that the exchange process was stopped for a limited concentration value (i.e. 10^{-3} N) characterized by a weak ions population in the case of Cu(II) and Co(II) cations [1].

On the other hand, Laird [14] has studied the influence of layer charge on smectite swelling and demonstrated that the increase in layer charge was accompanied by a decrease in crystalline swelling

* Corresponding author at: UR05/13-01, Physique des Matériaux Lamellaires et Nanomatériaux Hybrides (PMLNMH), Faculté des Sciences de Bizerte, Zarzouna 7021, Tunisia. Tel.: +216 20 843 705; fax: +216 72 590 566.
E-mail address: walidoueslati@ymail.com (W. Oueslati).

0169-4332/$ – see front matter © 2012 Elsevier B.V. All rights reserved.
http://dx.doi.org/10.1016/j.apsusc.2012.05.144

(smaller basal spacing values) characterized by an expansion in the size of smectite particles. The expansion of the interlamellar space is accompanied by a d_{001} basal spacing value fluctuation. Indeed, the study's of [15–20] investigates the dioctahedral smectite hydration properties using XRD profile modeling approach in order to assess the evolution of the water content in the interlamellar space under variable RH rates. They have shown that the increase in layer charge affects the transition from 2W to 1W (i.e. respectively two and one water layer hydration state) and from 1W to 0W (i.e. dehydrated layer).

In extension with earlier works [1], this study aims at characterizing the effect of an in situ applied hydrous strain (i.e. created with variable %RH rates) on the selective exchange process.

This process is developed when Na rich-montmorillonite is in contact with solutions containing (50%Cu^{2+}, 50%Co^{2+}) cations occurring from industrial wastewater, which impose a competitive ion exchange process. This problem often emerges if we want to apply clay properties as a natural geological membrane for a long period.

The choice of 50/50 for the Co^{2+}/Cu^{+2} ratio is adopted in order to compare obtained results, in the case of stressed sample, with an earlier study focusing unstressed ones [1]. This goal is achieved using XRD analysis with both its quantitative and qualitative analysis. The quantitative analysis consists in the comparison of experimental XRD patterns with theoretical ones and allows us to determine structural parameter characterizing structural changes along c^* axis.

2. Materials and methods

2.1. Starting materials

The starting materials are originated from bentonites of Wyoming. The <2 μm fraction of montmorillonite (SWy, Wyoming, USA) is supplied by the Source Clay Minerals Repository Collection [21]. This montmorillonite exhibits a low octahedral charge and extremely limited tetrahedral substitutions. The clay cation exchange capacity (CEC) is 101 mequiv./100 g [22].

2.2. Pretreatment

A pre-treatment of the starting material consists in preparing a Na-rich montmorillonite suspension. This process is assured by dispersing ~10 g of solid in ~100 mL of 1 M NaCl solution. Indeed, the SWy suspensions are shaken mechanically for 24 h in this saline solution before the separation of the solid fraction through centrifugation and the addition of fresh saline solution. These steps are repeated five times to ensure a whole cation exchange. The excess of salt is washed out in 24 h cycles, which include sedimentation, removal of the supernatant and immersion in deionized water. The obtained suspensions labeled as Swy-Na constitute the starting materials.

2.3. Experimental modeling of "in situ" hydrous strain

The"in situ" hydrous strain is created by varying content of water molecule in the environment of the studied sample (Swy-Na). This step is achieved by varying relative humidity rates using a diffractometer installation (Brüker D8-advance) and equipped with an Ansyco rh-plus 2250 humidity control device coupled to an Anton Paar TTK450 chamber. The relative humidity range extends from almost saturated condition (90%RH) to an extremely dry ones (10%RH). All XRD patterns are recorded following the same sequence of RHs, starting first from 10% up to 90% and then reducing RH to 10%. This step is repeated 15 times which means a series of 15 hydration–dehydration cycles. Based on XRD analysis, the expansion characteristics under variable RH rates is widely studied [18–20,23] revealing that the position of 0 0 1 basal reflections, which is shifted from the high angular 2θ range towards small ones, varied with the interlamellar water content.

By increasing of %RH amounts, smectite particles expand stepwise, with the different steps corresponding to the insertion of 0–3 sheets of H_2O molecules in the interlayer easily detected by X-ray diffraction by an increase in basal spacing.

2.4. Experimental modeling of the selectivity problem

The selectivity problem is simulated at the laboratory scale by dispersing the host material (i.e. Swy-Na) for 24 h in a solution containing (0.5Cu^{2+}, 0.5Co^{2+}) with various concentrations (10^{-1} N and 10^{-2} N). This process is developed for the unstressed starting sample and stressed ones (i.e. after applying hydrous strain). The obtained samples will be named respectively: *SWy-1N*, *SWy-2N*, *SWy-1N-S* and *SWy-2N-S*. An oriented film is prepared by the depositing of the obtained clay suspension onto a glass slide in order to get ready for XRD analysis.

2.5. XRD analysis

2.5.1. XRD equipment

All exchange process is monitored by qualitative XRD analysis. The XRD patterns were recorded using a Brüker D8-advance using Cu Kα monochromatic radiation. Usual scanning parameters were 0.02° 2θ as step size and 80 s as counting time per step over the angular range of 3–40° 2θ. The divergence slit, the two Soller slits, the antiscatter, and resolution slits were 0.5°, 2.3°, 2.3°, 0.5°, and 0.06°, respectively.

2.5.2. Qualitative XRD analysis

The qualitative analysis is based on a whole description of the experimental XRD profile along all explored 2θ range. This description is based on: the d_{001} basal spacing value, determined using EVA release Diffrac plus software (Bruker AXS GmbH, Karlsruhe, Germany), the FWHM (i.e. full width at half maximum intensity of 0 0 1 reflections) related to the 0 0 1 reflection which contain all structural information, the rationality of the reflection position which can be calculated using the Bailey [24] criteria and a global profile geometry description (i.e. symmetric and asymmetric X-ray peaks, identification of the supplementary reflection if they exist).

2.5.3. X-ray profile modeling method

The efficiency of XRD profile modeling approach in the investigation of hydrations properties and structural changes which accompanied any clay mineral perturbation was used and described by several works. The fitting strategy was detailed by [18,19] in the case of 00l reflections. Briefly, this method allowed us to determine structural characteristics along the normal to the (Z) plane. It consists on the comparison of the experimental X-ray patterns with theoretical ones calculated from structural models [2]. The method allowed determination of the number and the position of the exchanged cations and water molecules, the stacking layer thicknesses, the stacking mode along the normal to the layer plane. The theoretical diffracted intensity was given by the matrix formalism detailed by Drits and Tchoubar [2]:

$$I_{00}(2\theta) = L_p \,\mathrm{Spur}\left(Re[\phi][W]\left\{[I] + 2\sum_{n}^{M-1}\left[\frac{M-n}{n}\right][Q]^n\right\}\right)$$

where Re, indicates the real part of the final matrix; Spur, the sum of the diagonal terms of the real matrix; L_p, the Lorentz-polarization factor; M, the number of layers per stack; n, an integer varying between 1 and 1–M–1; [ϕ], the structure factor matrix; [I], the unit

Table 1
d_{001} basal spacing and FWHM value deduced from the qualitative XRD description in the case of stressed and unstressed Swy-Na sample.

Sample	Hydration process (increase of %RH)									Dehydration process (decrease of %RH)						
	10	20	30	40	50	60	70	80	90	80	70	60	50	40	30	20
Unstressed sample																
d_{001} (Å)	11.04	11.82	12.58	12.31	12.30/14.19	14.50	14.74	14.91	14.94	14.89	14.57	14.10	12.26/14.10	12.21	12.20	12.03
FWHM (2θ)	1.88	2.08	1.93	1.34	1.57	0.82	0.68	0.57	0.52	0.55	0.86	1.53	1.07	0.96	0.95	0.97
Stressed sample (after 15 hydration–dehydration cycles)																
d_{001} (Å)	11.84	11.98	11.57	11.71	12.05/12.76	14.66	14.74	14.91	15.01	14.91	14.88	14.44	12.59/13.84	12.33	12.22	12.13
FWHM (2θ)	1.43	1.72	1.63	1.48	1.57	0.72	0.66	0.54	0.51	0.52	0.57	1.03	1.64	1.44	1.05	0.84

matrix; [*W*], the diagonal matrix of the proportions of the different kinds of layers and; [*Q*], the matrix representing the interference between adjacent layers. This method allowed us to determine the abundances (W_i), the mode of stacking of the different kinds of layers and the mean number of layers per coherent scattering domain (CSD) [25,26]. Within a CSD, the stacking of layers is described by a set of junction probabilities (P_{ij}). The relationships between these probabilities and the abundances W_i of the different types of layers are given by Drits and Tchoubar [2]. Where P_{ij} is the probability of an *i* layer to be followed by a *j* layer.

During the simulation of the XRD patterns, some corrections must be taken into account, such as the Lorentz-polarisation factor and the preferred orientation [27,28]. The XRD patterns were calculated using the *Z* coordinates of Drits and Sakharov [29]. The origin of these coordinates was placed on the plane of surface oxygen atoms. For calculating structural model, a water molecule distribution in accordance with the literature's description was used [16,18,23].

2.6. CEC and specific surface area measurements

Under an appropriate condition, both surface areas and cation exchange capacities CEC of studied clay minerals (before and after applied hydrous strain) are measured using the method based on the absorption of methylene blue from aqueous solutions [30]. Indeed, methylene blue (MB) dye has been used to determine the surface area of clay minerals for several decades. The chemical formula is $C_{16}H_{18}C_lN_3S$, with a corresponding molecular weight of 319.87 g/mol. Methylene blue in aqueous solution is a cationic dye, $C_{16}H_{18}N_3S^+$, which absorbs to negatively charged clay surfaces. Hence, the specific surface of particles can be determined by the amount of absorbed methylene blue. The surface area covered by one methylene blue molecule is typically assumed to be 130 $Å^2$ (1 Å = 0.1 nm). It is important to highlight that the technique is done in water suspensions, thus expansive minerals can expose all available surface area. Specific surface is particularly relevant in the interpretation of a soil response that is significantly affected by surface processes, such as liquid limit, hydraulic and electrical conduction, chemical diffusion and atmospheric conditions.

3. Results and discussion

3.1. Qualitative XRD description

3.1.1. XRD investigation of unstressed sample

The hydration behavior of the unstressed sample is characterized using XRD analysis. We report in Fig. 1 experimental XRD patterns related to the first hydration–dehydration cycle. The results obtained from qualitative analysis, reported in Table 1, shows a hydration behavior in accordance with what has been found in previous works [31] related to the same sample specimen. Indeed, the evolution of the amounts of the interlamellar water molecule, in the Na rich montmorillonite, is reached through steps. Moreover, the transition "1W–2W" is obtained for RH rates between 40% and 60%. From high %RH value towards extremely saturated conditions (i.e. 90%RH), the sample remains characterized by 14.94 Å, d_{001} basal spacing value, which is attributed to a homogeneous "2W hydration state". In the downing dehydration cycle (Fig. 1), the same hydration behavior law is respected. But, a fast apparition of "1W hydration state," at70%RH, is noted and explained by a right broadening of the 0 0 1 reflection characterized by a 12.31 Å basal spacing value.

This hydration transition is completely achieved at 20%RH, which is logically interpreted by the hysteresis effect on the hydration–dehydration process. By lowering this RH range (i.e. <20%RH), a beginning of 0W layer hydration state appears, characterized by 11.04 Å d_{001} basal spacing value. The investigation of FWHM value (Table 1) shows that the intermediate hydration state, which accompanied all the hydration transition phases, is characterized by an interstratified hydration character recognized by the highest calculated value of FWHM and an irrational 00l reflection position.

3.1.2. XRD investigation of stressed sample

After 15 hydration–dehydration cycles, the stressed material is recorded under the same sequence of RHs.

The obtained experimental XRD patterns are reported in Fig. 2 and we summarize, in Table 1, all parameters deduced from the qualitative XRD analysis.

Indeed, for $70\% \leq RH \leq 90\%$ range, the studied sample present a 15.01 Å basal spacing value attributed to the homogeneous 2W hydration state. By lowering this RH rate towards extremely dried condition (10%RH), a heterogeneous hydration behavior is observed and characterized by a continuous hydration transition from 2W to 0W. This continuous transition was accompanied by a shift of d_{001} basal spacing value from 15.0 Å to 11.84 Å and with an increase in the FWHM value (Table 1) which can be explained by an interstratified hydration character. The same hydration behavior is observed by decreasing RH rate (Fig. 2). It is also noticed that there is a total absence of homogeneous 1W phases not even in room conditions (40%RH). This performance is probably due to the instability of the interlamellar space water molecule content which is affected by the intensity of the applied hydrous strain (i.e. number of hydration dehydration cycles). The final stressed materials behave as a homogeneous 2W hydrated state for RH > 70% and by lowering this RH range a dominant interstratified hydration character appears (Table 1).

3.2. Quantitative XRD description

Calculated and experimental profiles of unstressed and stressed Swy-Na samples are shown as a function of relative humidity in Figs. 1 and 2. The best agreement between theoretical and experimental XRD patterns is reached using several relative proportions of the different mixed-layer structures MLS. Proportions and compositions of the used MLS are reported in Tables 2 and 3.

Indeed, for unstressed Swy-Na sample three interlamellar water molecule configurations are used. That is to say, a random

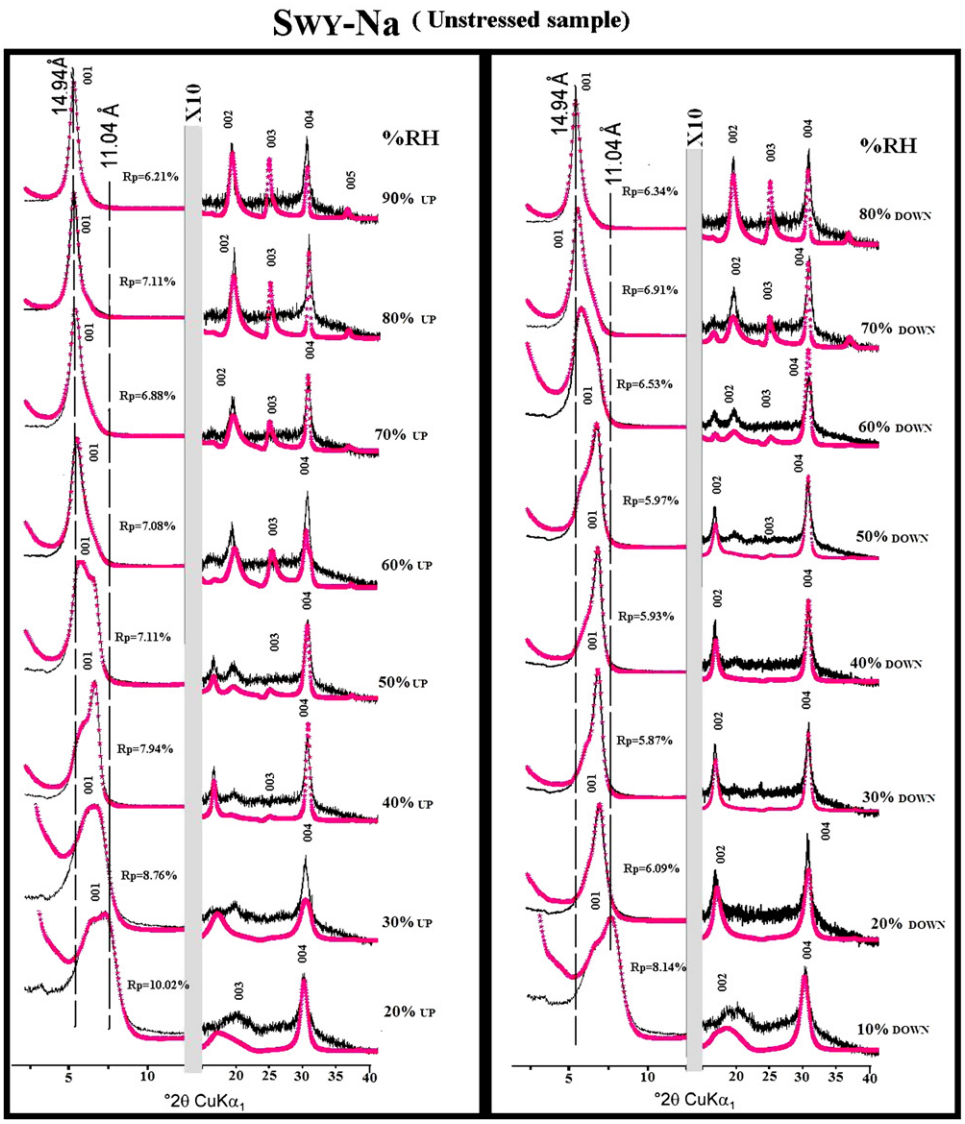

Fig. 1. Comparison between experimental and calculated XRD patterns as a function of %RH rate in the case of unstressed sample.

distribution of three types of layers (i.e. 0W, 1W and 2W) with the various abundance (see Table 2) are used. The water molecule distribution along c^* axis used to fit experimental data is in accordance with bibliographical data [16,18,23]. The average number of layers per "particle" [26] varied from 6 to 12.

The same explanation is well given for stressed Swy-Na sample (i.e. after 15 hydration dehydration cycle). Besides, we report in Table 3 all structural parameters obtained from the best agreement between theoretical and experimental XRD data.

This quantitative XRD investigation shows that all experimental profiles is simulated using a mixed layer structure, which indicates the existence of heterogeneous hydration behavior inspite of the qualitative description result. The average number of layers per particle varied from 7 to 10, thus, indicating a probable change in the crystallite size. We report in Fig. 3 the evolution of the theoretical relative proportions of 0W, 1W, and 2W layers, deduced from quantitative analysis, as a function of %RH rates, of the host and the final studied samples.

By comparing the evolution of "0W" phases for unstressed and stressed Swy-Na sample along the hydration process (i.e. by increasing RH rates) we show, in the case of unstressed materials (Fig. 3a), an obvious reduction in the 0W phases amount when %RH increases.

From 40%RH the dehydrated phases "0W" contribution become weak (≈0). The monohydrated phases (1W) present a maximum contributing value at room conditions (40%RH). However, these phases are always present, whether more or less than this RH value. This indicates, in its turn, the absence of a real homogeneous hydrated state. Concerning the bi-hydrated layer (2W) phases, there is an apparent increase versus %RH amounts. It presents a maximum contributing value for 90%RH, in which a minor contribution of 1W phases is introduced in the MLS.

For stressed Swy-Na sample, some change in the hydration behavior is noticed. Indeed, the contributions of the dehydrated layer (0W) in the MLS are present up to 60%RH (Fig. 3b). At 20%RH, the contribution of 0W phases decreases. This indicates that after 15 hydration dehydration cycles the interlamellar configuration has been changed and the amount of swelling clay fraction has been improved. As for monohydrated (1W) and bihydrated (2W) layer, a similar behavior is noticed with a weak variation in its mixed contribution at 90%RH in support of the 2W phases. Along the dehydration process (Fig. 3c and d) a similar profile evolution

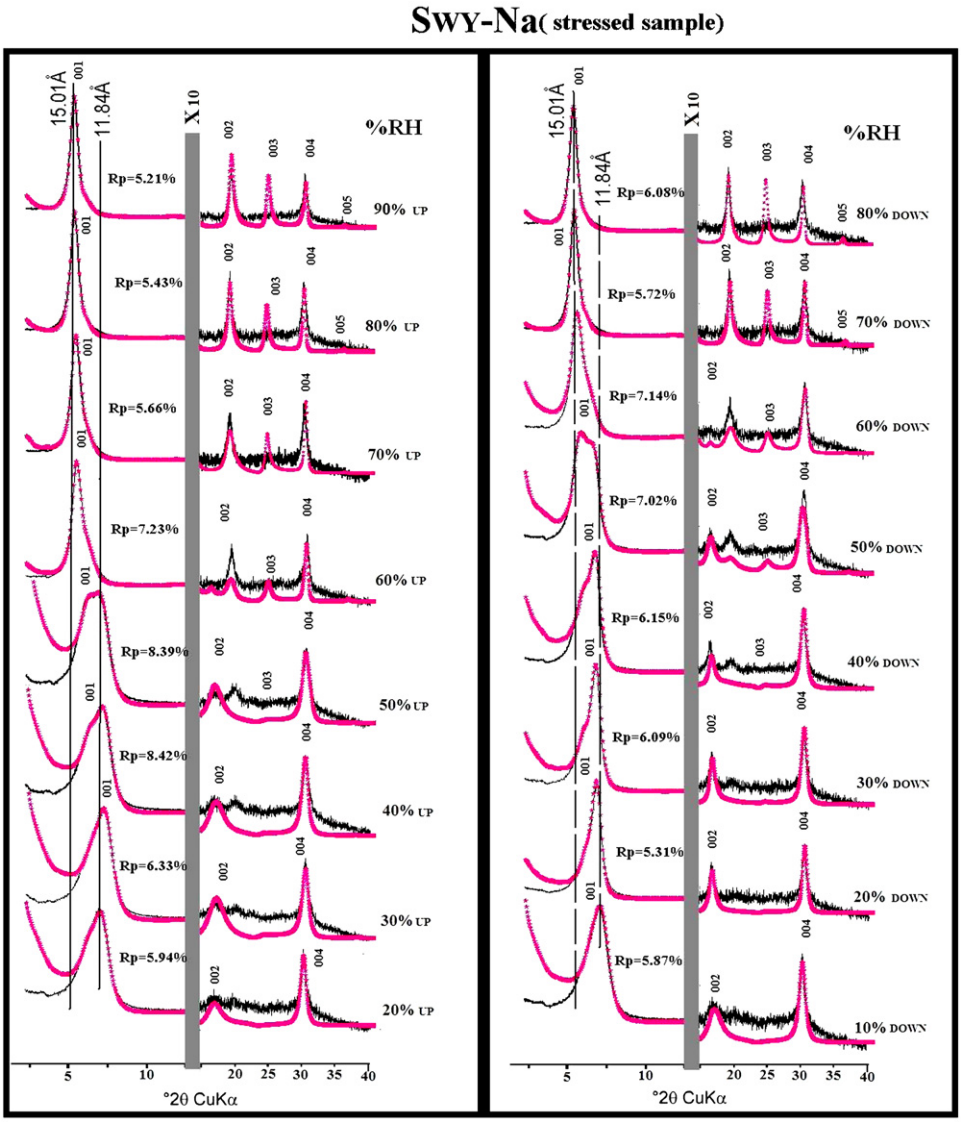

Fig. 2. Comparison between experimental and calculated XRD patterns as a function of %RH rate in the case of stressed sample.

for all hydration phases is observed. This evolution is characterized by a demixion of 1W and 2W phases for high RH value (i.e. from 70%RH for unstressed sample and from 60%RH for the stressed sample). For $40\% \leq RH \leq 60\%$ and for both samples, the structure was described by a major contribution of 1W phases randomly distributed with 2W and 0W phases. As regards to low RH value and in the case of unstressed materials, a reasonable amounts of water molecule sheets are used to describe the MLS, characterized by a major contribution of 0W phases, randomly distributed with 1W phases. Moreover, in the case of stressed material reported at 20%RH, we show that the XRD profile is modeled using a major contribution of 1W phases, demixed with a minor contribution of 0W phases. This remark is interpreted by a probable retained water molecule quantity in the interlamellar space after hydration dehydration cycles

3.3. XRD analysis of the selective exchange capacity (SEC)

3.3.1. Case of unstressed Swy-Na sample in contact with solution containing ($0.5Cu^{2+}$, $0.5Co^{2+}$)

The selectivity study of the Na-rich montmorillonite, in contact with a solution containing (Cu^{2+}, Co^{2+}) cation, is investigated by Oueslati et al. [1] using XRD profile modeling approach. They demonstrate that for high metals concentrations (i.e. 10^{-1} N) the host material is considered to be a homogeneous with 2W hydration state (i.e. 2W: two water sheet), characterized by d_{001} = 15.17 Å basal spacing value that is attributed to Co^{2+} cation. As for low normality, clay remains homogeneous with 1W hydration state, which is probably attributed to Na^{+} and/or Cu^{2+} cation. In this work the same problem, is focused, taking into account the presence of a hydrous strain caused by applying an "in situ" variation of the RH rates around the host material (i.e. Swy-Na). The experimental XRD patterns related to the unstressed sample, in contact with 10^{-1} N and 10^{-2} N solution, are reported in Fig. 4.

In the case of 10^{-1} N solution, the XRD pattern is characterized by d_{001} = 15.17 Å spacing. This indicates that the exchangeable sites are entirely saturated by Co^{2+}, which is characterized by 2W hydration state [18]. The irrationality of the reflections positions is explained using quantitative XRD analysis. Indeed, the best agreement is reached using theoretical model which consists in stacking two phases with variable proportion related, in a major contribution, to Co^{2+} cation with 87% (i.e. 2W) and Cu^{2+} cation with 13% (i.e. 1W) (Table 4). In the case of SWy-2N complex, an asymmetric 0 0 1 reflection characterized by two basal spacing values related

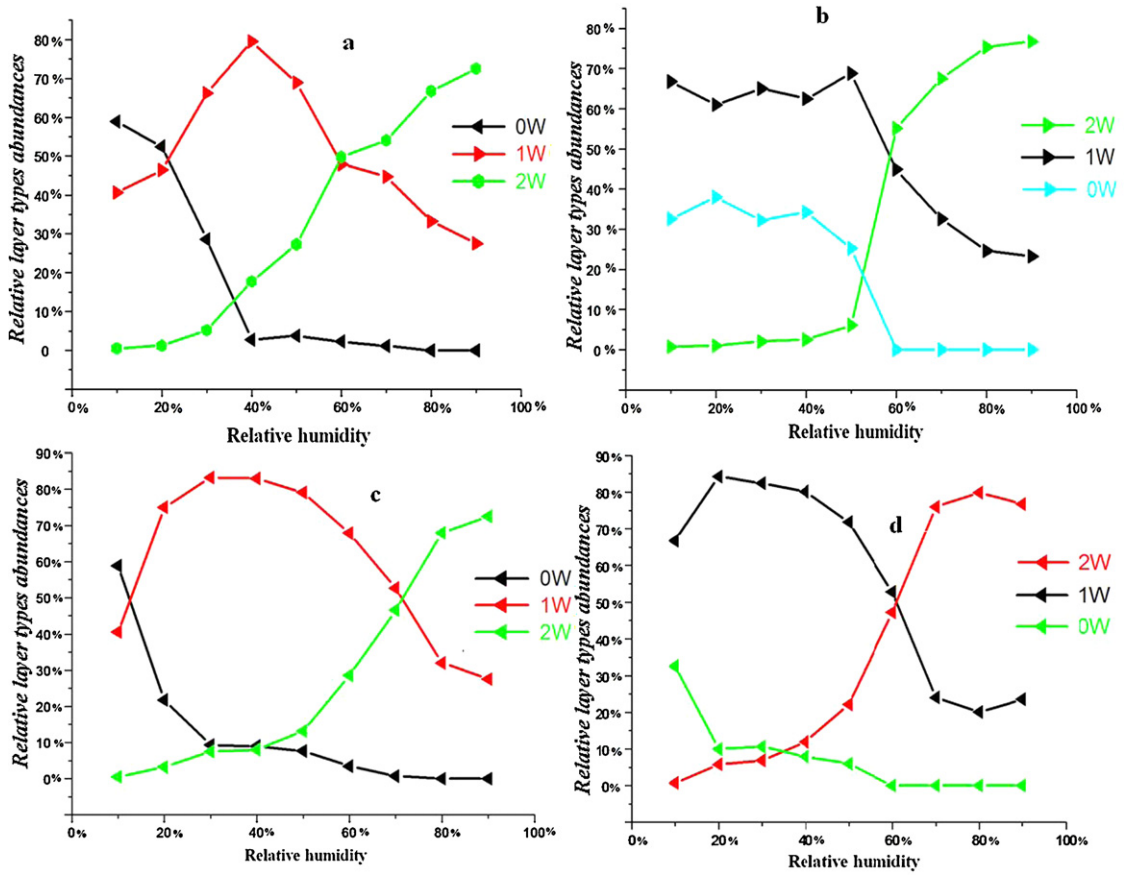

Fig. 3. Evolution of the relative contribution of the different layer types for: (a) unstressed SWy-Na sample along hydration process, (b) stressed along hydration process, (c) unstressed SWy-Na sample along dehydration process and (d) stressed along dehydration process.

respectively to 2W and 1 hydration state (i.e. d_{001} = 14.19 Å and d_{001} = 12.59 Å) is noted. The 2W hydration state existence is probably due to a partial presence of Co^{2+} cation in the interlamellar space. The irrationality of reflection position is interpreted by an interstratified character with a minor contribution of 1W phase (i.e. d_{001} = 12.59 Å) related to Cu^{2+} and/or Na^{+}. The best agreement between experimental and calculated profile is reported in Fig. 4. This agreement is reached using structural parameter summarized in Table 4.

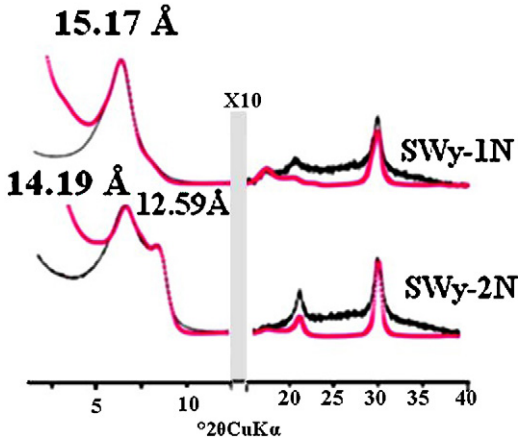

Fig. 4. Best agreement between experimental —- and theoretical *** XRD pattern obtained in the case of unstressed Swy-Na sample in contact with solution containing (0.5Cu^{2+}, 0.5Co^{2+}).

3.3.2. Case of stressed Swy-Na sample in contact with solution containing (0.5Cu^{2+}, 0.5Co^{2+})

In the case of 10^{-1} N and 10^{-2} N solution, the experimental XRD patterns related to the stressed Swy-Na sample (after 15 hydration dehydration cycles) are characterized, respectively, by 14.70 Å and 14.50 Å d_{001} basal spacing value (Fig. 5), attributed to a partial exchange with Co^{2+} cations [18]. All diffractograms present an asymmetric 00l reflection profile indicating the interstratified character. The quantitative XRD analysis shows that the MLS presents a random demixion between three hydration states (i.e. 0W, 1W and 2W).

For 10^{-1} N solution, the totality of the experimental XRD profile is reproduced using random demixion of 3.6% (0W), 59.4% (1W) and 37% (2W). The average number of layers per particle is 6. The presence of dehydrated layer (0W) on the structure after stress, can be explained by a new organization in the interlamellar space. For 10^{-2} N solution, the XRD profile is reproduced using 44% of (1W) phases related to Cu^{2+} cation randomly distributed with 56% of (2W) phases related to Co^{2+} cation. In general, for the sample undergoing an "in situ" hydrous perturbation, the ionic exchange process is altered and the sample exchange performance is improved. Indeed, stressed samples are characterized by an interstratified structure confirmed by the theoretical models which prove the coexistence of three types of MLS involving different hydration states due to the presence of more than one exchangeable cations in the interlamellar space (Co^{2+}, $Cu^{2+}$and may also Na^{+}). The theoretical water molecule distribution is in accordance with bibliographical data and the structural parameters deduced from the modeling approach are summarized in Table 4.

Table 2
Structural parameters used to reproduce experimental XRD patterns in the case of unstressed Swy-Na sample.

%RH	d_{001} (Å) (2W)	Z_n (Å) (Na^+)	nH_2o	Z_{H_2O} (Å)	d_{001} (Å) (1W)	Z_n (Å) (Na^+)	nH_2o	Z_{H_2O} (Å)	d_{001} (Å) (0W)	Z_n (Å) (Na^+)	%Abundance of layer type 0W//1W//2W	*M*
Hydration process (increase of %RH)												
10	15.40	12.60	2.40	10/14	12.15	11.20	1.20	09.70	09.70	08.90	58.9//40.6//0.5	7
20	15.60	12.60	2.40	10.3/14.2	12.25	11.20	1.20	09.70	09.65	08.90	52.44//46.36//1.2	7
30	15.00	12.60	2.60	10/14	12.25	11.20	1.30	09.70	09.95	08.90	28.56//66.24//5.2	6
40	15.20	12.60	4.40	10.2/14	12.30	11.20	1.80	09.70	10.20	08.90	2.75//79.5//17.75	11
50	15.20	12.60	5.00	10.2/14	12.40	11.20	2.00	09.30	10.20	08.90	3.8//68.9//27.3	10
60	15.00	12.60	5.60	10.5/14	12.40	11.20	2.80	09.70	10.20	08.90	2.25//47.95//49.8	9
70	15.35	12.60	5.60	10.35/14.1	12.40	11.20	2.80	09.70	10.30	08.90	12//44.75//54.05	10
80	15.45	12.60	5.80	10.5/14.2	12.45	11.20	2.80	09.00	–	08.90	0//33.25//66.75	12
90	15.35	12.60	5.80	10.6/14.2	12.40	11.20	2.80	09.00	–	08.90	0//27.5//72.5	11
Dehydration process (decrease of %RH)												
80	15.35	12.60	5.80	10.5/14.1	12.45	11.20	2.90	09.00	–	08.90	0//32//68	11
70	15.35	12.60	5.60	10.8/14.1	12.40	11.20	2.80	09.00	10.30	08.90	0.75//52.65//46.6	11
60	15.20	12.60	5.60	9.8/14	12.40	11.20	2.80	09.70	10.20	08.90	3.50//67.9//28.6	10
50	15.20	12.60	3.90	10.2/14	12.35	11.20	1.95	09.80	10.20	08.90	7.7//79.1//13.2	12
40	15.20	12.60	3.60	10.2/14	12.30	11.20	1.80	09.70	10.20	08.90	9//83//8	11
30	15.20	12.60	3.00	10/14	12.30	11.20	1.50	09.70	10.20	08.90	9.3//83.2//7.5	12
20	15.20	12.60	3.00	10/14	12.26	11.20	1.50	09.70	10.20	08.90	21.75//75//3.25	10

Table 3
Structural parameters used to reproduce experimental XRD patterns in the case of stressed Swy-Na sample.

%RH	d_{001} (Å) (2W)	Z_n (Å) (Na^+)	nH_2o	Z_{H_2O} (Å)	d_{001} (Å) (1W)	Z_n (Å) (Na^+)	nH_2o	Z_{H_2O} (Å)	d_{001} (Å) (0W)	Z_n (Å) (Na^+)	%Abundance of layer type 0W//1W//2W	*M*
Hydration process (increase of %RH)												
10	15.50	12.60	2.4	9/14	12.20	11.20	1.2	9.8	9.7	08.90	32.55/66.75/7	7
20	15.50	12.60	3	9.1/13.9	12.10	11.20	1.5	9.8	9.6	08.90	38/61/1	7
30	15.50	12.60	3	9/14	12.30	11.20	1.5	9.8	9.7	08.90	32.2/65.8/2	7
40	15.50	12.60	3.2	9.2/14	12.15	11.20	1.6	10	9.65	08.90	34.2/62.5/2.5	7
50	14.80	12.60	3.6	9/14	12.15	11.20	1.8	10	9.65	08.90	25.2/68.76/6.04	6
60	15.20	12.60	5	10/14	12.40	11.20	1.8	10.3	–	08.90	0/44.9/55.1	10
70	15.25	12.60	5.8	10.2/14	12.30	11.20	2.4	9.7	–	08.90	0/32.5/67.5	8
80	15.35	12.60	6.4	10.2/14.2	12.55	11.20	2.7	9.9	–	08.90	0/24.64/75.36	10
90	15.35	12.60	7.4	10.2/14.2	12.55	11.20	3	9.7	–	08.90	0/23.25/76.25	9
Dehydration process (decrease of %RH)												
80	15.30	12.60	7	10.3/14	12.45	11.20	3	9.9	–	08.90	0/20.13/79.87	9
70	15.20	12.60	6.4	10.2/14	12.45	11.20	2.8	9.7	–	08.90	0/24/76	10
60	15.10	12.60	6	9.9/14	12.38	11.20	2.5	9.8	–	08.90	0/52.8/47.2	7
50	15	12.60	5.8	9.8/14	12.40	11.20	2.2	10	10.2	08.90	6/71.8/22.2	8
40	15.20	12.60	5	10/14.2	12.30	11.20	2	9.7	10.3	08.90	7.9/80.20//11.9	8
30	15.20	12.60	4.4	10.2/14	12.30	11.20	1.9	9.9	10.2	08.90	10.65/82.5/6.85	9
20	15	12.60	4	10/14	12.25	11.20	1.3	9.7	10	08.90	10/84.25/5.75	10

Table 4
Optimum structural parameters used to fit the experimental XRD profile related respectively to SWy-1N, SWy-2N, SWy-1N-S and SWy-2N-S samples.

Sample	d_{001} (Å) (2W)	Z_n (Å) (Co^{2+})	nH_2O	Z_{H_2O}	d_{001} (Å) (1W)	Z_n (Å) (Cu^{2+})	nH_2O	Z_{H_2O}	d_{001} (Å) (0W)	Z_n (Å) (Na^+)	%Abundance of layer type 0W//1W//2W[a]	*M*
SWy-1N	15.20	12.60	1.90	13.90/11.30	12.40	11.20	1.10	11.20	–	–	0//13//87	6
SWy-2N	15.20	12.60	1.90	13.90/11.30	12.40	11.20	1.10	11.20	–	–	0//35//65	7
SWy-1N-S	14.70	12.50	6.4	10.50/14.50	12.40	9.50	1.10	9.50	10.30	8.9	03.6//59.4//37	6
SWy-2N-S	14.50	12.50	6.4	9.60/14.20	12.40	9	1.10	9	–	–	0//44//56	7

Z_n: position of exchangeable cations per half unit cell calculated along c^* axis; nH_2O: number of H_2O molecule per half unit cell; Z_{H_2O}: position along c^* axis of H_2O molecule; *M*: average layer number per stacking.
[a] A random succession layer type law probability is used for all theoretical models. From Ref. [18].

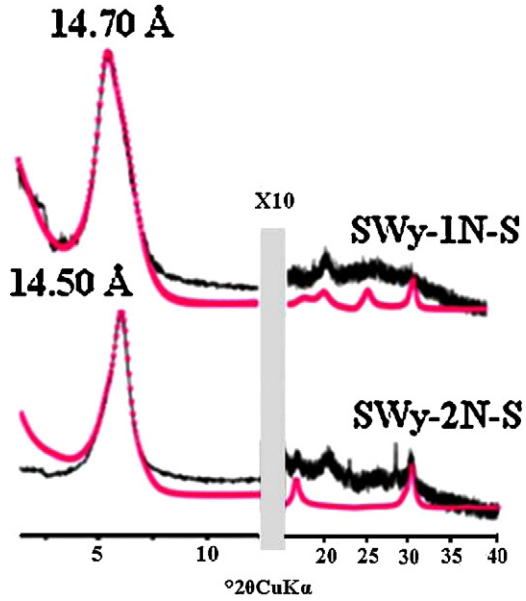

Fig. 5. Best agreement between experimental–- and theoretical*** XRD pattern obtained in the case of stressed Swy-Na sample in contact with solution containing ($0.5Cu^{2+}$, $0.5Co^{2+}$).

Table 5
CEC and specific surface area measurement before and after applying hydrous strain.

Sample	CEC (mequiv./100 g) clay	Surface area (m^2/g) of clay
Unstressed sample	101	750
Stressed sample	53.33	436

3.4. Cation exchange capacity (CEC) and surface area (SA) measurement

In order to determine the effect of the applied hydrous strain on the intrinsic cation exchange properties of montmorillonite, we conduct a measurement of the CEC and the specific surface area respectively before and after applying hydrous constraint. We report in Table 5 the obtained results and we show a remarkable change in the CEC value which decreases from 101 to 53.33 mequiv./100 g clay, thus, indicating the lessening of the exchangeable site in the host materials after stress. The specific surface area decreases from 750 to 436 m^2/g, indicating major changes in the morphological geometry of the studied complex. This results can be attributed to the new organization of the interlamellar space content.

4. Conclusion

In this work we try to characterize the strain effect, that is produced by a continuous hydration–dehydration cycles, using "in situ" variation of %RH rate, on the cationic exchange process in the case of Na rich-montmorillonite (Swy-2). In this regard, the final results show: (1) a similar hydration behavior, of stressed and unstressed materials, characterized by an interstratified hydration character for RH ≤ 60% rates. (2) After 15 hydration dehydration cycles, the observed structural change is characterized by a decrease in the amount of exchangeable sites. (3) The selective exchange process is developed for both stressed and unstressed materials. (4) For low concentration (10^{-2} N), all samples are characterized by an interstratified hydration character with a major contribution of 2W phase related to a partial saturation with Co^{2+} cations. (5) For high concentration (10^{-1} N), all samples are

characterized by an interstratified hydration state and the d_{001} spacing values are attributed, in major part, to the Co^{2+} and Cu^{2+} cations for SWy-2 and SWy-S, respectively. (6) The intrinsic clay properties (i.e. CEC, specific surface area) which characterize Na-rich montmorillonite is affected by applying hydrous strain.

Acknowledgements

The manuscript was much improved by the constructive reviews of anonymous reviewers. The editorial assistance of Federico Rosei (Appl Surf Sci) is acknowledged.

References

[1] W. Oueslati, M. Meftah, R. Chalghaf, H. Ben Rhaiem, A. Ben Haj Amara, XRD investigation of selective exchange process for di-octahedral smectite: case of solution saturated by Cu^{2+} and Co^{2+} cation, Zeitschrift für Kristallographie Proceedings 1 1 (2011) 389–395.
[2] V.A. Drits, C. Tchoubar, X-ray Diffraction by Disordered Lamellar Structures: Theory and Applications to Microdivided Silicates and Carbons, Springer-Verlag, Berlin, 1990.
[3] A. Viani, A.F. Gualtieri, G. Artioli, The nature of disorder in montmorillonite by simulation of X-ray powder patterns, American Mineralogist 87 (7) (2002) 966–975.
[4] H. Ben Rhaiem, A. Ben Haj Amara, J. Ben Brahim, C.H. Pons, Quantitative analysis of XRD and SAXS patterns: determination of the mineralogy and microstructure of Ca-interstratified clays, Materials Science Forum 278–281 (1998) 868–872.
[5] P. Barré, C. Montagnier, C. Chenu, L. Abbadie, B. Velde, Clay minerals as a soil potassium reservoir: observation and quantification through X-ray diffraction, Plants and soil 302 (2008) 213–220.
[6] C.H. Zhou, Z.F. Shen, L.H. Liu, S.M. Liu, Preparation and functionality of clay-containing films, Journal of Materials Chemistry 21 (2011) 15132–15153.
[7] C.H. Zhou, Emerging trends and challenges in synthetic clay-based materials and layered double hydroxides, Applied Clay Science 48 (1–2) (2010) 1–4.
[8] F. Claret, B.A. Sakharov, V.A. Drits, B. Velde, A. Meunier, L. Griffault, Clay minerals in the meuse haute marnes underground laboratory: possible influence of organic matter on clay mineral evolution, Clays and Clay Minerals 52 (2004) 515–532.
[9] M. Rousseau, L. Di Pietro, R. Angulo-Jaramillo, D. Tessier, B. Cabibel, Preferential transport of soil colloidal particles: physicochemical effects on particle mobilization, Vadose Zone Journal 3 (2004) 247–261.
[10] S. Lantenois, B. Lanson, F. Muller, A. Bauer, M. Jullien, A. Plançon, Experimental study of smectite interaction with metal Fe at low temperature: 1 smectite destabilization, Clays and Clay Minerals 53 (2005) 597–612.
[11] W. Oueslati, H. Ben Rhaiem, B. Lanson, A. Ben Haj Amara, Selectivity of Na-montmorillonite in relation with the concentration of bivalent cation (Cu^{2+}, Ca^{2+} Ni^{2+}) by quantitative analysis of XRD patterns, Applied Clay Science 43 (2009) 224–227.
[12] G. Huang, J. Gao, X. Wang, Preparation and characterization of montmorillonite modified by phosphorus–nitrogen containing quaternary ammonium salts, Applied Surface Science 258 (2012) 4054–4062.
[13] M. Borisover, N. Bukhanovsky, I. Lapides, S. Yariv, Thermal treatment of organoclays: effect on the aqueous sorption of nitrobenzene on *n*-hexadecyltrimethyl ammonium montmorillonite, Applied Surface Science 256 (2010) 5539–5544.
[14] D.A. Laird, Influence of layer charge on swelling of smectites, Applied Clay Science 34 (2006) 74–87.
[15] K. Tamura, H. Yamada, H. Nakazawa, stepwise hydration of high-quality synthetic smectite with various cations, Clays and Clay Minerals 48 (2000) 400–404.
[16] E. Ferrage, B. Lanson, N. Malikova, A. Plançon, B.A. Sakharov, V.A. Drits, New insights on the distribution of interlayer water in Bi-hydrated smectite from X-ray diffraction profile modeling of 0 0 l reflections, Chemistry of Materials 17 (2005) 3499.
[17] F. Hubert, L. Caner, A. Meunier, B. Lanson, Advances in characterization of soil clay mineralogy using X-ray diffraction: from decomposition to profile fitting, European Journal of Soil Science 60 (2009) 1093–1105.
[18] W. Oueslati, H. Ben Rhaiem, A. Ben Haj Amara, XRD investigations of hydrated homoionic montmorillonite saturated by several heavy metal cations, Desalination 271 (2011) 139–149.
[19] E. Ferrage, B. Lanson, L.J. Michot, J.L. Robert, Hydration properties and interlayer organization of water and ions in synthetic Na-smectite with tetrahedral layer charge part 1. Results from X-ray diffraction profile modeling, Journal of Physical Chemistry C 114 (2010) 4515–4526.
[20] I. Bérend, J.M. Cases, M. François, J.P. Uriot, L.J. Michot, A. Masion, F. Thomas, Mechanism of adsorption and desorption of water vapor by homoionic montmorillonites; 2, the Li^+-, Na^+-, K^+-, Rb^+- and Cs^+-exchanged forms, Clays and Clay Minerals 43 (1995) 324–336.
[21] W.F. Moll, Baseline studies of the clay minerals society source clays: geological origin, Clays and Clay Minerals 49 (5) (2001) 374–380.
[22] G.W. Brindley, T. Suzuki, M. Thiry, Interstratified kaolinite–smectite from the Paris Basin; correlation of layer proportions, chemical compositions, and other data, Bulletin of Minerals Information 106 (1983) 403–410.
[23] T. Sato, T. Watanabe, R. Otsuka, Effects of layer charge, charge location, and energy change on expansion properties of dioctahedral smectites, Clays and Clay Minerals 40 (1992) 103–113.
[24] S.W. Bailey, Nomenclature for regular interstratifcations, American Mineralogist 67 (1982) 394.
[25] J. Mering, L'interférence des rayons X dans les systèmes à stratification désordonée, Acta Crystallographica 2 (1949) 371.
[26] H. Ben Rhaïem, D. Tessier, A. Ben Haj Amara, Mineralogy of the <2 μm fraction of three mixed-layer clays from southern and central Tunisia, Clay Minerals 35 (2000) 375–381.
[27] R.C. Reynolds, The Lorentz-polarization factor and preferred orientation in oriented clay aggregates, Clays and Clay Minerals 34 (1986) 359–367.
[28] A. Ben Haj Amara, J. Ben Brahim, A. Plançon, H. Ben Rhaïem, Étude par Diffraction X des Modes d'Empilement de la Nacrite Hydratée et Deshydratée, Journal of Applied Crystallography 31 (1998) 654–662.
[29] V.A. Drits, B.A. Sakharov, X-ray Structure Analysis of Mixed-Layer Minerals, Nauka, Moscow, 1976.
[30] N. Yener, C. Biçer, M. Önal, Y. Sarıkaya, Simultaneous determination of cation exchange capacity and surface area of acid activated bentonite powders by methylene blue sorption, Applied Surface Science 258 (2012) 2534–2539.
[31] W. Oueslati, M.S. Karmous, H. Ben Rhaiem, B. Lanson, A. Ben Haj Amara, Effect of interlayer cation and relative humidity on the hydration properties of a dioctahedral smectite, Zeitschrift fur Kristallograhie Suppl. 26 (2007) 417–422.